

RSC Advances



This is an *Accepted Manuscript*, which has been through the Royal Society of Chemistry peer review process and has been accepted for publication.

Accepted Manuscripts are published online shortly after acceptance, before technical editing, formatting and proof reading. Using this free service, authors can make their results available to the community, in citable form, before we publish the edited article. This *Accepted Manuscript* will be replaced by the edited, formatted and paginated article as soon as this is available.

You can find more information about *Accepted Manuscripts* in the [Information for Authors](#).

Please note that technical editing may introduce minor changes to the text and/or graphics, which may alter content. The journal's standard [Terms & Conditions](#) and the [Ethical guidelines](#) still apply. In no event shall the Royal Society of Chemistry be held responsible for any errors or omissions in this *Accepted Manuscript* or any consequences arising from the use of any information it contains.

Balanced strength and ductility improvement of in situ crosslinked polylactide/poly(ethylene terephthalate glycol) blends

Rui-Ying Bao, Wen-Rou Jiang, Zheng-Ying Liu, Wei Yang, Bang-Hu Xie, Ming-Bo Yang*

College of Polymer Science and Engineering, Sichuan University, State Key Laboratory of Polymer Materials
Engineering, Chengdu, 610065, Sichuan, China

Abstract

Poly(lactide) (PLA) is strong and stiff but brittle while poly(ethylene terephthalate glycol) (PETG) is flexible. In view of their complementary properties, PETG was blended with PLA via reactive melt blending to overcome the drawbacks of PLA, aiming at the applications in packaging industries. During reactive blending, crosslinking reaction between PLA chains and methylene diphenyl diisocyanate (MDI) led to improved melt elasticity, viscosity and molecular mass evaluated by various rheological plots including storage and loss modulus, viscosity, loss tangent, weighted relaxation spectra, and molecular weight distribution curves. Interfacial compatibilization occurred between PLA and PETG through the reaction of free isocyanate groups on crosslinked PLA chains with the terminal hydroxyl groups of PETG chains. The variation of viscoelasticity of PLA matrix and interfacial compatibilization resulted in fine phase morphology and enhanced interfacial adhesion of the blends. Thus, the failure mode of the blends changed from brittle fracture of neat PLA to ductile fracture. The resulted PLA-MDI/PETG blends displayed significantly improvement in the elongation at break and a simultaneous improvement of tensile strength, maintaining the high tensile modulus.

* Corresponding author. Tel.: + 86 28 8546 0130; fax: + 86 28 8546 0130.

E-mail address: weiyang@scu.edu.cn (W Yang)

1. Introduction

Poly(lactide) (PLA), as a biodegradable polymer with high strength and modulus, is potential to be widely used in areas such as biomedical devices, packaging, disposable tableware, fibers, and consumer goods.¹⁻⁶ However, practical application of PLA is significantly restricted by its inherent brittleness, as evidenced by the limited elongation at break. Plasticizers are frequently used to increase the flexibility and ductility of PLA. To be useful, plasticizers must decrease the glass transition temperature of the polymer, meaning the plasticizer and polymer must be miscible. Plasticizers, including poly(ethylene glycol) (PEG), poly(propylene glycol) (PPG) and poly(ethylene oxide) (PEO) were investigated and they all showed similar results with good improvements in elongation at break but a significant reduction in the tensile modulus and tensile strength at the meanwhile.⁷⁻¹² More importantly, these binary blends had high tendency to lose mechanical properties with time at ambient temperature due to easy migration of plasticizers.

Furthermore, various flexible polymers, such as poly(butylene succinate) (PBS), poly(butylene adipate-*co*-terephthalate) (PBAT), and polyhydroxy butyrate (PHB) have been introduced into PLA with the goal of enhancing the ductility, only to find limited promotion of ductility but greatly reduced strength and stiffness.^{13, 14} The blends prepared by simple blending suffer from lower fracture properties due to serious phase separation and poor interfacial adhesion between the immiscible components. An effective approach to improve the compatibility of polymer blends is reactive blending.¹⁵⁻²⁴ Therefore, in situ reactive blending is preferred for blending PLA with various polymers to improve its properties. The flexible phase can be in situ crosslinked for better comprehensive performance of the blends, and ductile PLA blends can be obtained by crosslinking

of flexible polymer and interfacial compatibilization. Wang et al.^{25, 26} prepared PLA/crosslinked polyurethane (PLA/CPU) with CPU dispersed in PLA matrix via reactive blending of PLA with poly(ethylene glycol) (PEG) and polymeric methylene diphenylene diisocyanate (PMDI). The in situ polymerization of PEG and PMDI in PLA matrix formed CPU, and interfacial compatibilization between PLA and CPU phases occurred owing to the reaction of NCO groups with terminal hydroxyl groups of PLA. Fang et al.²⁷ successfully prepared PLA materials consisting of PLA and cross-linked poly(ethylene glycol) diacrylate (PEGDA) by in situ reactive melt blending of PLA and PEG-based diacrylate monomer with no addition of any exogenous radical initiators. While significant improvement in tensile elongation has been realized, maintaining the high tensile strength and modulus of PLA is still difficult. Consequently, the applications of such blends in packaging industries are still limited. For PLA, like other brittle thermoplastics, an important goal is to increase the elongation at break without adversely affecting the tensile strength and tensile modulus.

Poly (ethylene terephthalate glycol) (PETG), namely, poly (ethylene- co-1,4-cyclohexanedimethanol terephthalate), is a random copolymer of poly(ethylene terephthalate) (PET) with an additional 30-34 mol% of 1,4-cyclohexanedimethanol (CHDM).²⁸ The presence of bulky CHDM group in the main chain makes PETG an amorphous thermoplastic of PET family. Mechanical properties of PETG are close to those of PET and PETG shows good flexibility, degradability, gas barrier properties, and processability without the need to use any additives.²⁹ Excellent gas barrier properties make it an outstanding choice for storing environmentally sensitive materials. Nowadays, PETG is used in medical, pharmaceutical and cosmetic packaging. Recently, PETG has been used to blend with PLA via melt blending to overcome the drawbacks of PLA,

aiming at the applications in packaging industries.^{28,30} Wang et al.³¹ studied the effect of dispersed phase morphology on the porous structure of PLA/PETG blend foams using multi-functional epoxide as reactive compatibilizer. More homogeneous and finer porous morphology of PLA/PETG foams with high expansion ratio could be achieved with a proper content of compatibilizer.

The performance of an immiscible polymer blend not only depends on the physical characteristics of its components, but also highly on the phase interface and phase morphology formed during mixing process in melt-blended samples, both of which are closely associated with the viscoelasticity of the polymer components. However, to the best of our knowledge, there is no report dealing with the effect of crosslinking of matrix on the properties of PLA blends, though the dispersed flexible phase is usually in situ crosslinked for better comprehensive performance of the blends as mentioned above. In this work, the crosslinking of PLA matrix by methylene diphenyl diisocyanate (MDI) changed the viscoelasticity of matrix greatly, and in situ compatibilization by MDI improved the interfacial adhesion between PLA and PETG phase. The results showed that the elongation at break of PLA/PETG blends in presence of MDI was significantly improved, and the tensile strength was enhanced without deterioration in the tensile modulus.

2. Experimental Section

2.1 Materials and sample preparation

Commercial PLA (trade name 2003D) with a density of 1.26 g/cm³ was purchased from NatureWorks LLC. PETG, with a density of 1.27 g/cm³, was obtained from Eastman Kodak Chemical Company. The weight-average molecular weight of PLA and PETG are 170 kg/mol and 70

kg/mol, respectively (determined by gel permeation chromatography). MDI (trade name 44V20L) was obtained from Bayer Co., Germany.

PLA and PETG were vacuum dried at 60 °C for 12 h before use. All the blends were prepared with a Haake Rheometer (Haake Rheomix 600, Germany) at 180 °C and 60 rpm. Typically, PLA and MDI were first reactive blended for 5 min, then a certain amount of PETG was added into the mixing chamber and blended for another 5 min. For all the samples, the weight ratio of PLA to PETG was kept at 80:20. The weight ratio of MDI shifted from 0, to 1, 3 and 5 wt% of the weight of PLA. For convenience, the specimens were denoted as PLA-xMDI/PETG, where x represent the content of MDI. In order to study the effect of MDI on the properties of PLA, PLA and MDI were also reactive blended in the chamber for 5 min. When there was no PETG, the obtained samples were marked as PLA-xMDI, where x also represent the content of MDI. For comparison, neat PLA was also processed under the same conditions. These samples were compression molded at 180 °C and 10 MPa for 4 min, then cold pressed with water cooling at 10 MPa for 3 min before ejecting the samples. Prior to compression molding, the pellets prepared from the blended polymers were dried in a vacuum oven at 60 °C for 8 h.

2.2 Characterizations and measurements

The linear rheological tests were performed on a stress-controlled dynamic rheometer AR2000ex (TA Instruments) with a 25 mm-parallel plate geometry and a gap of 1200 μm. A Rheology Advantage Software program, specially designed for AR Rheometers, was used for the system control, data collection and analysis. The samples for rheological measurement were compression molded into sheet (thickness = 2 mm) at 180 °C under 10 MPa. The samples were dried

in vacuum at 60 °C for 6 h before measurement. The measurements were carried out in a frequency range of 0.01-100 Hz at 180 °C under nitrogen atmosphere for neat PLA, PLA-MDI and its blends with PETG. Stress sweep was carried out to determine the limit on the strain for linear viscoelastic response, and 150 Pa oscillatory stress sweep was used.

Crosslinked PLA is insoluble in dichloromethane, so PLA-MDI and PLA-MDI/PETG samples were extracted in soxhlet apparatus using dichloromethane as the solvent. In this way, the crosslinked PLA could be separated, and then dried for fourier transform-infrared spectroscopy (FTIR) measurement. FTIR spectra were recorded on a Nicolet 6700 FTIR spectrometer (Nicolet Instrument Company, USA) equipped with an attenuated total reflectance (ATR) accessory in a range of wavenumbers from 4000 to 400 cm^{-1} . FTIR spectra were obtained by adding 32 scans at a resolution of 2 cm^{-1} .

The gel fraction in the crosslinked PLA-MDI was measured. The samples with weight W_1 were extracted in soxhlet apparatus at 50 °C for 12 h, and dichloromethane was used as the solvent. The obtained insoluble products were dried for 48 h in 60 °C vacuum oven and weighed (W_2). The gel fraction (f) was calculated from the following equation:

$$\text{Gel fraction (\%)} = (W_2 / W_1) \times 100 \quad (1)$$

The specimens for tensile tests were prepared by cutting compression molded sheets with a thickness of 0.3 mm into dog-bone type samples (4 mm width \times 20 mm gauge length \times 0.3mm thickness). Tensile tests were conducted at room temperature with an Instron-5567 universal testing machine (Instron, Canton, MA, USA) according to ASTM D638, and the crosshead speed was 1 mm min^{-1} . At least five specimens were tested for each sample, and the averaged result was reported.

The morphologies of blends were examined by FEI-INSPECTF scanning electron microscopy (SEM, Hillsboro, OR, USA) at an accelerating voltage of 5 kV. The compression molded sheets were cryofractured in liquid nitrogen, and the fractured surfaces were sputter-coated with a thin layer of gold prior to examination. The fractured surfaces after tensile test were also observed using the same SEM apparatus.

The particle size of PETG phase dispersed in PLA matrix was analyzed using an Image-Pro Plus software. For each specimen, at least 300 particles from several independent SEM micrographs were measured. The number-average particle size (d_n), weight-average particle size (d_w) and particle size distribution parameter (σ) were calculated from the following equations:

$$d_n = \frac{\sum_{i=1}^N n_i d_i}{\sum_{i=1}^N n_i} \quad (2)$$

$$d_w = \frac{\sum_{i=1}^N n_i d_i^2}{\sum_{i=1}^N n_i d_i} \quad (3)$$

$$\ln \sigma = \sqrt{\frac{\sum_{i=1}^N n_i (\ln d_i - \ln d)^2}{\sum_{i=1}^N n_i}} \quad (4)$$

where n_i is the number of PETG particles with the diameter of d_i . In the case of monodispersity, σ is equal to 1, and when there is polydispersity, σ is greater than 1.

3. Results and Discussion

3.1 Structural characterization

Rheological properties

Fig. 1 shows storage modulus and loss modulus (G' and G'') of neat PLA and PLA-MDI/PETG blends. As shown in Fig. 1, increasing content of MDI improved G' and G'' of PLA-MDI/PETG

blends. With the content of MDI increasing to 3 wt%, G' approached to G'' at low frequency region, indicating that the elasticity was enhanced obviously. With the content of MDI increasing to 5 wt%, G' was higher than G'' over the entire frequency range, indicating the dominance of elastic responses over viscous responses. For the polymer blends, it could be ascribed to the formation of crosslinking network with high crosslinking density.

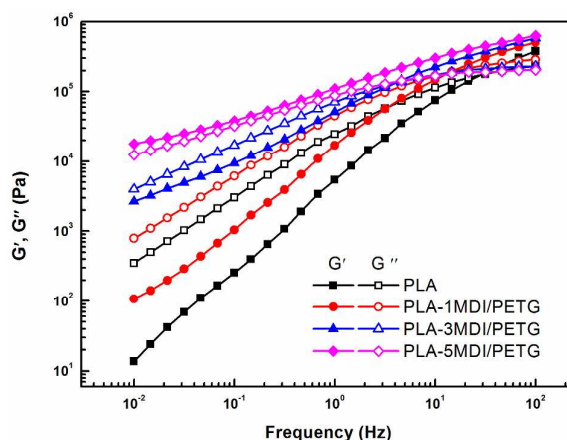


Fig. 1 storage modulus and loss modulus (G' and G'') of neat PLA and PLA-MDI/PETG blends.

Considering during the preparation, PLA and MDI were first reactive blended in the chamber, rheological responses of PLA-MDI were further studied in detail to provide abundant information regarding chain structures. Fig. 2 shows the frequency dependences of storage and loss modulus (G' and G''), complex viscosity ($|\eta^*|$) and loss tangent ($\tan \delta$) for neat PLA and PLA-MDI. As shown in Fig. 2(a), increasing content of MDI led to greatly improved G' and G'' of PLA-MDI, which could be ascribed to the formation of PLA crosslinking network that restricted the mobility of the polymer chains. With the content of MDI increasing to 3 wt%, G' approached to G'' at low frequency region, indicating that elasticity enhanced obviously. With the content of MDI increasing to 5 wt%, G' was even higher than G'' over the entire frequency range, indicating the dominance of elastic responses over viscous responses due to the high crosslinking density. As shown in Fig. 2(b), the typical

Newtonian plateau at low frequencies was observed for neat PLA. $|\eta^*|$ increased distinctly with content of MDI increasing, which was also ascribed to the increased crosslinking density of PLA. It was reported that the presence of crosslinks or entangled networks in a polymer melt could increase the viscosity.³² The Newtonian plateau disappears and shear thinning could be observed at low frequencies for PLA-3MDI and PLA-5MDI, indicating the dramatic increased viscosity induced by crosslinking. The viscosity data was fitted by Cross equation³³

$$\eta = \eta_0 / [1 + (\tau_0 \dot{\gamma})^{1-n}] \quad (5)$$

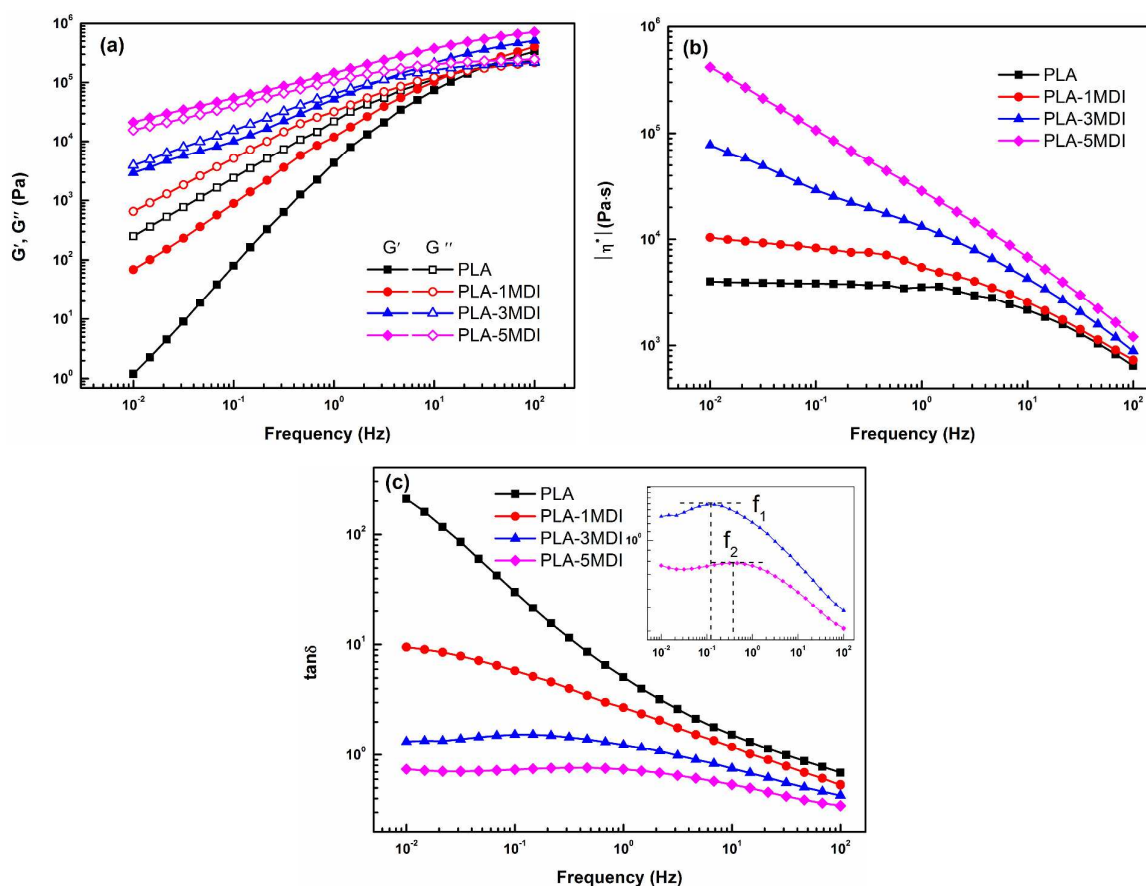


Fig. 2 Variation of (a) storage and loss modulus (G' and G''), (b) complex viscosity ($|\eta^*|$) and (c) loss tangent ($\tan \delta$) as functions of frequency for neat PLA and PLA-MDI.

where η_0 is the zero shear viscosity, τ_0 the characteristic relaxation time, and n is an exponent. Table 1 shows the zero shear viscosity of neat PLA, PETG, and PLA-MDI. A significant increase in the zero shear viscosity was realized in PLA-MDI, compared with that of neat PLA. The zero shear viscosity increased with the content of MDI increasing. The viscosity ratio of dispersed phase to matrix (η_d/η_m) decreased obviously due to the increase of viscosity of PLA induced by crosslinking.

Table 1. Zero shear viscosity of neat PLA, PETG, and PLA-MDI.

	neat PLA	PLA-1MDI	PLA-3MDI	PLA-5MDI	Neat PETG
$\eta_0(\text{Pa}\cdot\text{s})$	3.91×10^3	1.04×10^4	1.07×10^5	6.07×10^5	1.72×10^4
Viscosity ratio(η_d/η_m)	4.40	1.65	0.16	0.03	—

Tan δ ($\tan \delta = G''/G'$) is an essential parameter characterizing the relaxation behavior of the viscoelastic materials and is regarded to be more sensitive to the relaxation changes than G' and G'' . As shown in Fig. 2(c), tan δ of neat PLA decreased with increasing frequency, which was a typical behavior for viscoelastic liquid. With increasing content of MDI, tan δ decreased gradually, indicating that the reaction between PLA and MDI restrained the relaxation of polymer chains. For PLA-3MDI and PLA-5MDI, a tan δ peak at low frequencies, an indicator of the dominant elastic response of the melt, could be observed. This could be ascribed to that the network structure owing to crosslinking induced the transition from the liquid-like to solid-like viscoelastic behaviors. These results clearly indicated that a network has been formed in the PLA-MDI melt with increasing content of MDI. The transition from the liquid-like to solid-like viscoelastic behaviors at low frequencies also demonstrated that the long-range polymer chains motion was restrained by the formed crosslinking network significantly. Moreover, as shown by the inset of Fig. 2(c), the frequency showing tan δ peak ($f_2=0.33\text{Hz}$) for PLA-5MDI was higher than that of PLA-3MDI

($f_1=0.12\text{Hz}$), indicating the network structure for PLA-5MDI was more compact than that of PLA-3MDI, i.e, the crosslinking density for PLA-5MDI was higher than that of PLA-3MDI.

NLREG technique was used to convert the dynamic properties into continuous relaxation, $H(\lambda)$ spectra through³⁴

$$G' = \int_{-\infty}^{\infty} \frac{\omega^2 \lambda^2}{1 + \omega^2 \lambda^2} H(\lambda) d \ln \lambda \quad (6)$$

$$G'' = \int_{-\infty}^{\infty} \frac{\omega \lambda}{1 + \omega^2 \lambda^2} H(\lambda) d \ln \lambda \quad (7)$$

where ω (rad/s) is the angular frequency, and λ is the relaxation time. The weight relaxation spectrum $\lambda H(\lambda)$ are shown in Fig. 3. As shown in Fig. 3, the relaxation time increased with increased MDI content. The relaxation time of PLA-1MDI (0.07s) was longer than that of neat PLA (0.02s), and also

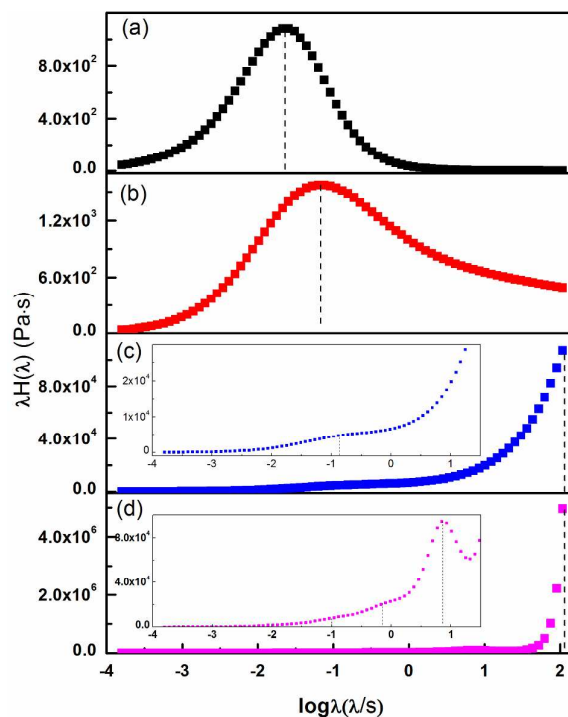


Fig. 3 Weighted relaxation spectra of PLA-MDI samples: (a) neat PLA, (b) PLA-1MDI, (c) PLA-3MDI, and (d) PLA-5MDI.

the relaxation peak got wider, indicating that the crosslinking of PLA induced by MDI restrained the relaxation of polymer chains. As the content of MDI increased to 3 and 5 wt%, PLA chains could not relax completely in the test frequency range, and the long time relaxation peak was incomplete. However, one and more short-time relaxation peaks (marked by dash line as shown in the inset of Fig. 3(c) and (d)) appeared before the long-time relaxation peak for PLA-3MDI and PLA-5MDI, respectively. The appearance of multiple relaxation times suggested the formation of branching structures^{35,36}, which delayed the relaxation of polymer chains significantly.

To effect the transformation of $H(\lambda)$ into the distribution of molecular weight, $w(M)$, an approximation formula based on the double reptation rule was used. The basic equation was the (generalized) mixing rule:³⁷

$$G_{rept}(t) = G_N \left(\int_{M_e}^{\infty} F(M, t)^{1/\beta} w(M) \frac{dM}{M} \right)^\beta \quad (8)$$

where G_N is the plateau modulus, and M_e is the entanglement molecular weight. $F(M, t)$ denotes the relaxation kernel function, which describes the relaxation behavior of a molecular weight fraction with a molecular weight of M , and β is a parameter which characterizes the mixing behavior. The subscript *rept* of the stress relaxation $G(t)$ indicates that only the contribution of the reptation dynamics of the whole polymer chain are considered, the dynamics of the chain segments (Rouse modes), which are only weakly dependent on $w(M)$, are not considered. The molecular weight distribution curves of PLA-MDI samples with different contents of MDI obtained from rheological analysis are shown in Fig. 4. The obtained molecular parameters, number-average molecular mass (M_n), weight-average molecular mass (M_w), and the polydispersity index (PDI) are listed in Table 2. With the content of MDI increasing, the curves shifted to the higher molecular weight region

possibly due to the chain branching. Moreover, an evident shoulder could be seen at high molecular weight position for all other samples prepared by reacting with MDI. It also could be seen that both M_n and M_w increased with increasing MDI content, and PDI also increased. Multiple peaks could be observed on the curves of PLA-5MDI, also indicating the formation of branching structure, which was in consistent with the results of relaxation time.

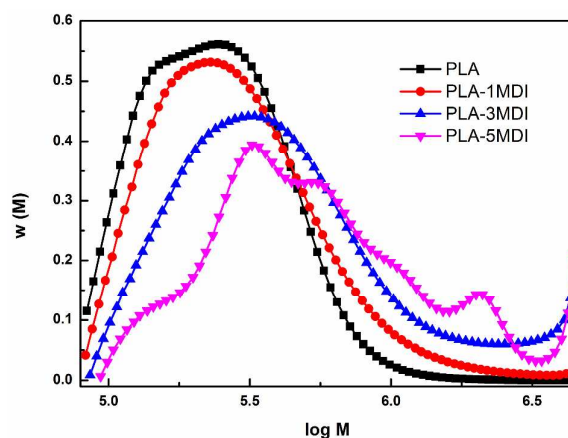


Fig. 4 The molecular weight distribution curves of PLA-MDI samples with different contents of MDI obtained from rheological analysis.

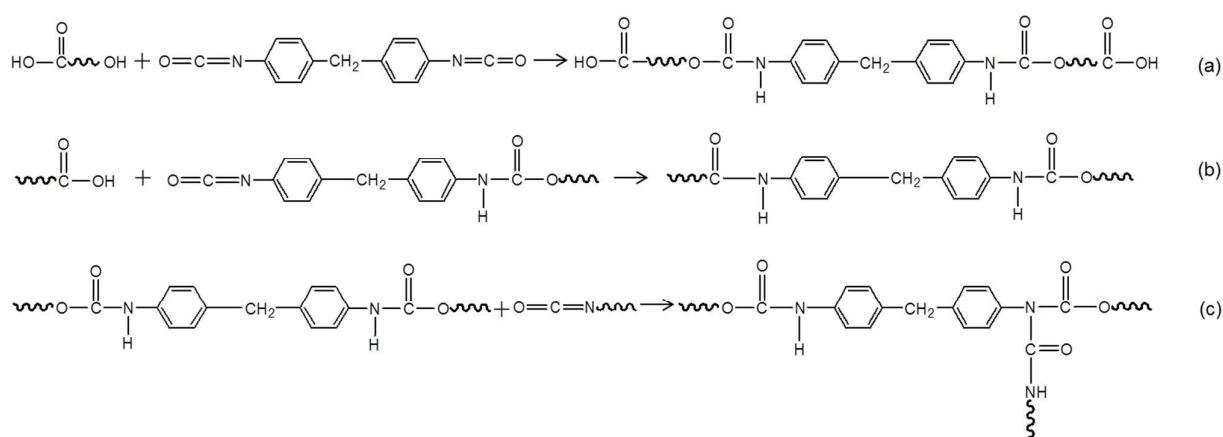
Table 2. The parameters of molecular weight for PLA/MDI samples obtained from rheological data.

	neat PLA	PLA-1MDI	PLA-3MDI	PLA-5MDI
$M_n/\text{g mol}^{-1}$	2.1×10^5	2.3×10^5	3.1×10^5	4.1×10^5
$M_w/\text{g mol}^{-1}$	2.8×10^5	3.7×10^5	6.3×10^5	9.5×10^5
PDI	1.4	1.6	2.1	2.3

Reaction mechanism

It is reported that isocyanate group of MDI can connect the hydroxyl end groups of PLA molecules through carbamate bonds, and the reaction of chain extension occurs as shown in Scheme 1(a).¹⁸ Because PLA had a very high molecular weight, terminal hydroxyl groups in the PLA was extremely low. The feed molar ratio of NCO of MDI to OH of PLA was much higher than 1 : 1, and

the excess amount of the isocyanate group might also react with the other end of PLA molecule ($-\text{COOH}$) to form amide linkage according to reaction Scheme 1(b) or react with the urethane group known as an allophanate reaction³⁸ to cause chain branching or crosslinking as shown in Scheme 1(c).^{39, 40} Gel fraction was measured to confirm the crosslinking reactions in PLA during melt-blending. Table 3 gives the changes in gel fraction of PLA with increasing MDI content. The gel fraction of PLA increased dramatically from 11.7 % to 51.4 % with the MDI content up to 5wt%.



Scheme 1. Reaction mechanism for chain extension and chemical crosslinking of PLA with MDI.

Table 3. Gel fraction of PLA-MDI samples with different contents of MDI.

PLA-MDI samples	PLA-1MDI	PLA-3MDI	PLA-5MDI
Gel fraction(%)	11.7	35.9	51.4

FTIR spectra of dichloromethane extracted PLA-MDI were recorded and compared with that of neat PLA, as shown in Fig. 5(a). All the characteristic PLA absorption peaks could be observed in the spectrum of PLA-MDI. Compared with neat PLA, some new absorption peaks could be found in the spectrum of PLA-MDI blends. The two new absorption peaks around 1540 and 1600 cm^{-1} were ascribed to the characteristic absorptions of N–H bond, conjugated double bonds of benzene ring, respectively, suggesting the reaction between PLA and MDI during blending. Moreover, the

characteristic absorption peak of isocyanate group (-NCO) at around 2270 cm^{-1} could be detected in the spectra of PLA-MDI samples, indicating that free isocyanate groups existed in PLA-MDI samples during blending.

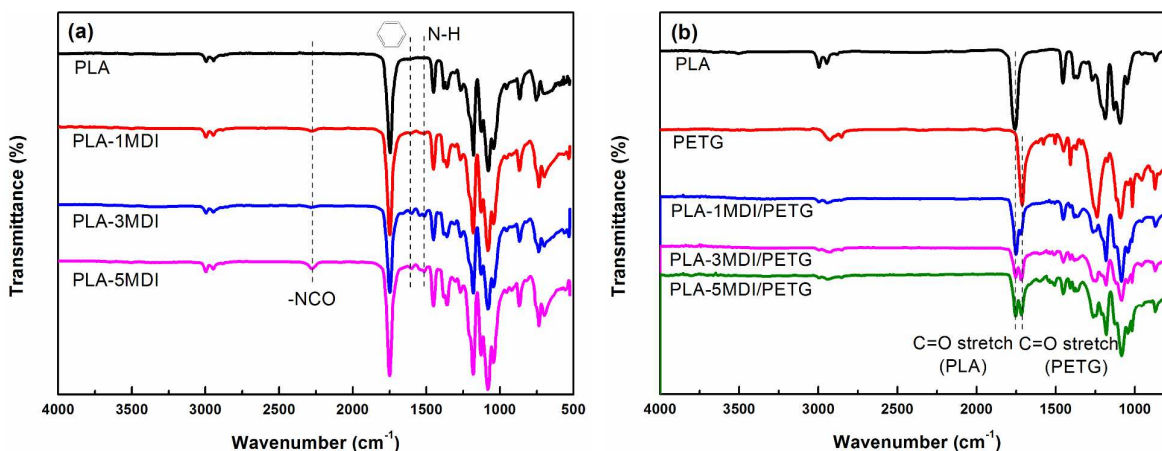


Fig. 5 FTIR spectra of (a) neat PLA, and dichloromethane extracted PLA-MDI with different contents of MDI, and (b) neat PLA, neat PETG, and dichloromethane extracted PLA-MDI/ PETG with different contents of MDI

The interfacial compatibilization would take place between PLA matrix and PETG phase through the reaction of free isocyanate groups on crosslinked PLA with the terminal hydroxyl groups of PETG. The FTIR spectra of dichloromethane extracted PLA-MDI/PETG were recorded and compared with that of neat PLA and PETG, as shown in Fig. 5(b). The peaks at 1758 cm^{-1} and 1712 cm^{-1} were the C=O stretch of PLA and PETG, respectively. Both the peaks at 1758 and 1712 cm^{-1} ascribing to PLA and PETG appeared in PLA-MDI/PETG samples, indicating that crosslinked PLA-co-PETG copolymer was formed in situ between crosslinked PLA and PETG. With the content of MDI increasing to 3 and 5 wt%, the peak intensity of 1712 cm^{-1} ascribing to C=O stretch of PETG increased and was close to that of 1758 cm^{-1} ascribing to C=O stretch of PLA, possibly due to the larger amounts of crosslinked PLA-co-PETG copolymer formed. Moreover, the characteristic absorption at around 2270 cm^{-1} of free isocyanate groups existed in PLA-MDI samples disappeared

for PLA-MDI/PETG blends. Thus, we could conclude that the active free isocyanate groups on crosslinked PLA could connect the –OH of PETG and PLA to form the crosslinked PLA-co-PETG copolymer. The crosslinked PLA-co-PETG copolymer could reduce the interfacial tension and increased the interfacial adhesion, thus acting as a compatibilizer.

3.2 Mechanical properties

Typical stress-strain curves of neat PLA, PLA/PETG blend and PLA-MDI/PETG blends with different amounts of MDI are present in Fig. 6(a). PLA was very rigid and showed a high tensile strength, but the elongation at break of about 7% indicated that it undergone brittle fracture. The simple PLA/PETG blend was even more brittle than neat PLA, and showed even lower tensile strength because of very weak interface adhesion between PLA and PETG. With the addition of MDI, the strength of the PLA-MDI/PETG blends increased obviously. The PLA-MDI/PETG blends showed initial strain softening after yielding and then undergone stable neck growth and a brittle to ductile transition occurred due to the presence of MDI. Because PETG was more flexible that could deform easily under tensile stress, and the interfacial interaction between PETG phase and PLA phase was stronger due to in situ compatibilization, remarkable plastic deformation of PLA matrix could be brought by the presence of MDI. The tensile strength, elongation at break, and tensile modulus of neat PLA, PLA/PETG blend and PLA-MDI/PETG blends are shown in Fig. 6(b-d), and the performances of PLA-MDI samples are also displayed considering the effect of the variation of matrix on the properties of blends. Different from the low tensile strength of PLA/PETG blend, the tensile strength of PLA-MDI/PETG blends was much higher than that of neat PLA and PETG, due to the increased tensile strength of PLA-MDI matrix induced by crosslinking and the enhanced

interface adhesion, rather than the improvement of crystallinity. It was confirmed that the crosslinking of PLA chains resulted in the decreased crystallization ability of PLA from Fig. S1 and Table S1. It was more interesting to note that, compared with the greatly reduced elongation at break of simple PLA/PETG blend, the elongation at break of PLA-MDI/PETG blends was significantly improved though the ductility of PLA-MDI matrix deteriorated due to the crosslinking. The elongation at break of the PLA-3MDI/PETG blend increased to 96%, nearly 13 times higher than neat PLA, as shown in Fig. 6(c). Moreover, a high tensile modulus could be maintained for PLA-MDI/PETG blends as shown in Fig. 6(d).

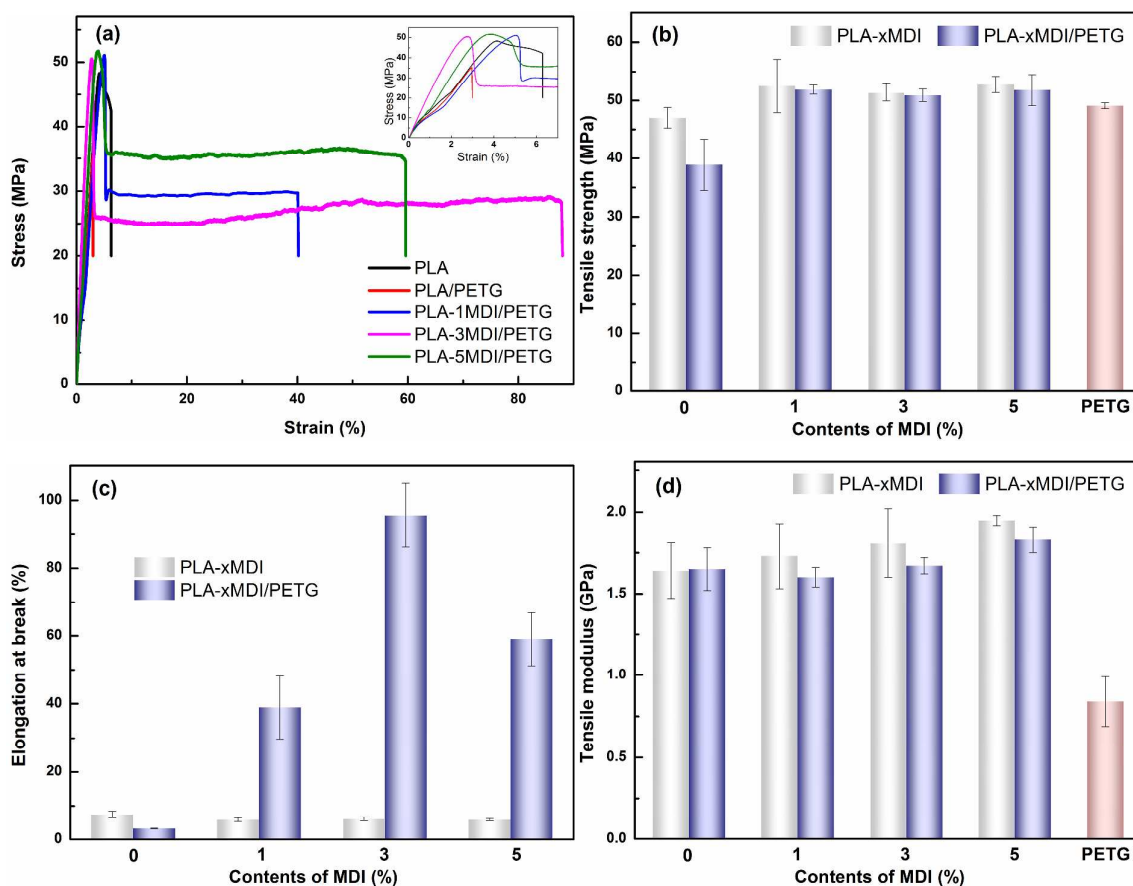


Fig. 6 (a) tensile stress-strain curves, (b) tensile strength, (c) elongation at break, and (d) tensile modulus of PLA and PLA/PETG blends modified by MDI at room temperature.

3.3 Phase morphology

SEM micrographs of cryogenic fractured surfaces and corresponding d_n distributions of the blends are shown in Fig. 7. All the blends exhibited a phase-separated morphology with PETG particles dispersed in PLA matrix, and finer phase morphology (smaller PETG particles size with narrower size distribution) could be seen in the blends with MDI. To make a clear comparison, the statistical results of the PETG particle size and its distribution are summarized in Table 4. A substantial decrease in the particle size and its distribution could be observed in the blends with MDI, possibly due to the variation of viscosity ratio between matrix and dispersed phase. The increase in viscosity of PLA matrix could contribute to the morphology refinement by preventing aggregation of PETG particles. The compatibility between PLA and PETG was poor as evidenced by the obvious interfacial voids between PETG particles and PLA matrix. However, after the addition of MDI, the interface cracks of PLA-MDI/PETG blends disappeared. The principal cause for the improvement of compatibility could be attributed to the in situ formation of crosslinked PLA-co-PETG copolymer at the interface of two immiscible polymers. The in situ reaction between the isocyanate group of MDI on crosslinked PLA and hydroxyl groups of PETG resulted in crosslinked PLA-co-PETG copolymers containing carbamate linkages. The finer phase morphology and the enhanced interfacial adhesion by crosslinked interfaces were important contributing factors on significantly improved mechanical properties. Bhardwaj and Mohanty⁴¹ reported that hydroxyl functional hyperbranched polymer (HBP) was in situ cross-linked in PLA matrix. The prepared blends showed about 850% improvements in elongation at break, and remarkably maintained high strength and modulus values,

attributing to the fine dispersion of HBP phase and formation of crosslinked interfaces between HBP phase and PLA matrix.

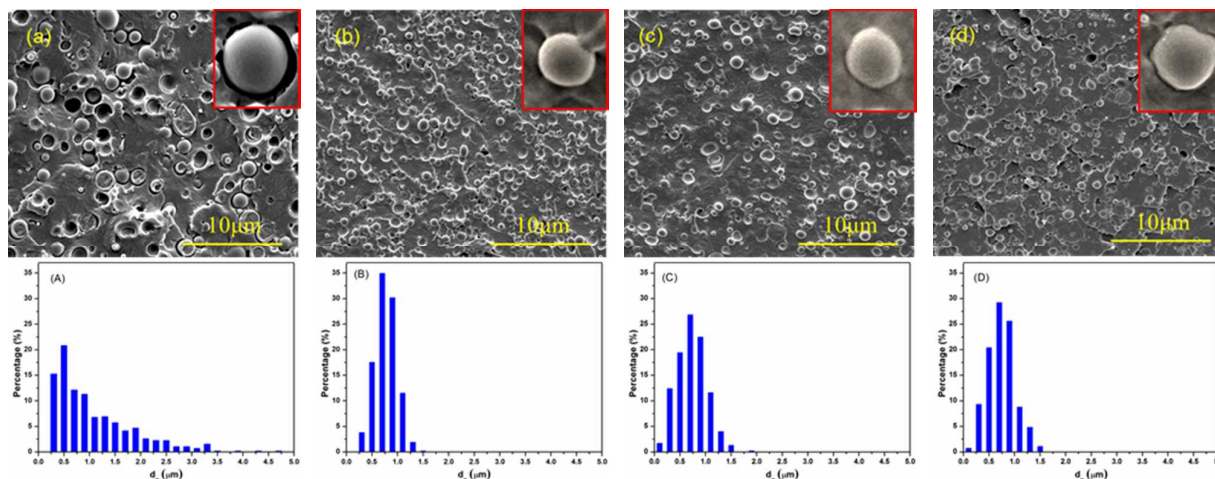


Fig. 7 SEM micrographs of cryo-fractured surfaces and the corresponding d_n distributions of the blends: (a, A) PLA/PETG, (b, B) PLA-1MDI/PETG; (c, C) PLA-3MDI/PETG and (d, D) PLA-5MDI/PETG.

Table 4. Weight-average particle size (d_w), number-average particles size (d_n), and particles size distribution parameter (σ) of PETG dispersed phase for PLA-MDI/PETG blends.

sample	$d_w(\mu\text{m})$	$d_n(\mu\text{m})$	σ
PLA/PETG	1.61	1.07	2.00
PLA-1MDI/PETG	0.83	0.77	1.36
PLA-3MDI/PETG	0.85	0.73	1.64
PLA-5MDI/PETG	0.83	0.74	1.50

Fig. 8 shows SEM micrographs of tensile-fractured surfaces of the blends. The tensile-fractured surface of neat PLA was flat and smooth, indicating neat PLA undergone brittle fracture. For PLA/PETG blends, interfacial debonding between PLA and PETG phases were clearly observed, but no perceptible deformation of PETG or PLA matrix occurred. It suggested that the PLA/PETG blends undergone brittle failure as well. Since the interfacial adhesion between PLA and PETG was

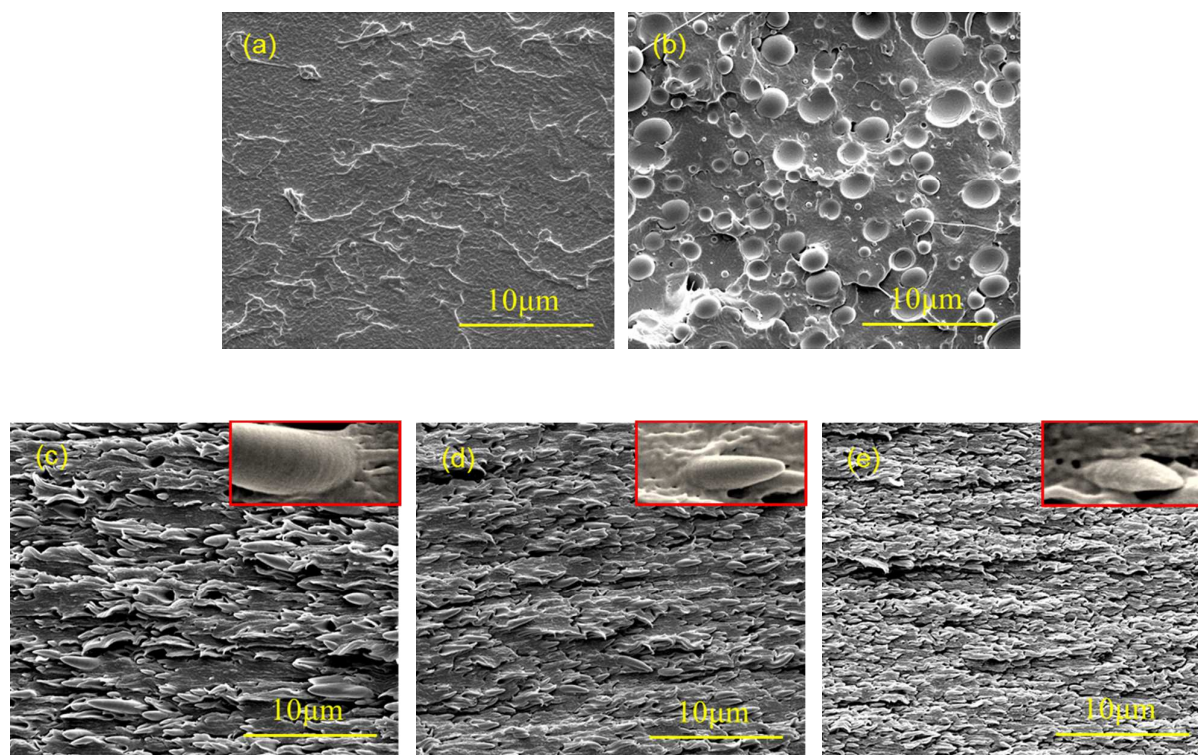


Fig. 8 SEM micrographs of tensile-fractured surfaces of the blends: (a) PLA, (b) PLA/PETG, (c) PLA-1MDI/PETG; (d) PLA-3MDI/PETG and (e) PLA-5MDI/PETG.

weak, the smooth surface depicted easy debonding of the phases during fracture. On the other hand, the tensile-fractured surface of PLA-MDI/PETG blends exhibited highly elongated PETG fibrils and a large degree of matrix deformation, indicating that a brittle-to-ductile transition occurred. During tensile process, PETG particles, which had much lower elastic modulus than PLA matrix, could deform easily and would effectively induce matrix shear yielding under the support of excellent interfacial interaction. Good interfacial adhesion was kept between deformed PETG phase and shear yielded PLA matrix, and the deformed PETG could not debond from PLA matrix as shown in the magnified pictures at the top right of Fig. 8(c-e). It suggested that the deformed PETG particles

could promote localized plastic deformation of PLA matrix and caused effective energy dissipation during tensile fracture process.

4. Conclusion

PLA blends with balanced strength and ductility improvement were successfully prepared by reactive melt blending with PETG in the presence of MDI. The crosslinking of PLA matrix by MDI increased the melt elasticity and viscosity of matrix greatly, and compatibilization of the in situ formed crosslinked PLA-co-PETG copolymer improved the interfacial adhesion between PLA matrix and PETG phase, leading to a 13-time improvement of elongation at break of PLA-MDI/PETG blends. The tensile strength of the blends was improved simultaneously, and the tensile modulus was maintained. This work provides a potential technique to increase the elongation at break without adversely affecting the tensile strength and tensile modulus of PLA materials, which is helpful for enlarging the applications of PLA in packaging industries.

Acknowledgment

This work was supported by the National Natural Science Foundation of China (NNSFC Grants 51422305 and 21374065), the Major State Basic Research Development Program of China (973 program) (2012CB025902), Sichuan Provincial Science Fund for Distinguished Young Scholars (2015JQ0003) and the Innovation Team Program of Science & Technology Department of Sichuan Province (Grant 2014TD0002).

References

- 1 V. Ojijo and S. S. Ray, *Prog. Polym. Sci.* 2013, **38**, 1543-1589.

- 2 R. E. Drumright, P. R. Gruber and D. E. Henton, *Adv. Mater.* 2000, **12**, 1841-1846.
- 3 L. T. Lim, R. Auras and M. Rubino, *Prog. Polym. Sci.* 2008, **33**, 820-852.
- 4 G. Liu, X. Zhang and D. Wang, *Adv. Mater.* 2014, **26**, 6905-11.
- 5 P. A. Delgado and M. A. Hillmyer, *RSC Adv.* 2014, **4**, 13266-13273.
- 6 P. Ma, P. Xu, W. Liu, Y. Zhai, W. Dong, Y. Zhang and M. Chen, *RSC Adv.* 2015, **5**, 15962-15968.
- 7 W.-C. Lai, W.-B. Liao and T.-T. Lin, *Polymer* 2004, **45**, 3073-3080.
- 8 Y. Hu, M. Rogunova, V. Topolkarayev, A. Hiltner and E. Baer, *Polymer* 2003, **44**, 5701-5710.
- 9 Z. Kulinski, E. Piorkowska, K. Gadzinowska and M. Stasiak, *Biomacromolecules* 2006, **7**, 2128-2135.
- 10 Z. Kulinski and E. Piorkowska, *Polymer* 2005, **46**, 10290-10300.
- 11 K. S. Anderson, K. M. Schreck and M. A. Hillmyer, *Polymer Reviews* 2008, **48**, 85-108.
- 12 A. J. Nijenhuis, E. Colstee, D. W. Grijpma and A. J. Pennings, *Polymer* 1996, **37**, 5849-5857.
- 13 L. Jiang, M. P. Wolcott and J. Zhang, *Biomacromolecules* 2005, **7**, 199-207.
- 14 K. Zhang, A. K. Mohanty and M. Misra, *ACS Appl. Mater. Inter* 2012, **4**, 3091-3101.
- 15 H. Liu, F. Chen, B. Liu, G. Estep and J. Zhang, *Macromolecules* 2010, **43**, 6058-6066.
- 16 H. Z. Liu, W. J. Song, F. Chen, L. Guo and J. W. Zhang, *Macromolecules* 2011, **44**, 1513-1522.
- 17 H. Liu, L. Guo, X. Guo and J. Zhang, *Polymer* 2012, **53**, 272-276.
- 18 X. Li, H. Kang, J. Shen, L. Zhang, T. Nishi, K. Ito, C. Zhao and P. Coates, *Polymer* 2014, **55**, 4313-4323.
- 19 V. Ojijo, S. S. Ray and R. Sadiku, *ACS Appl. Mater. Inter* 2013, **5**, 4266-4276.
- 20 H. Z. Liu and J. W. Zhang, *J. Polym. Sci. Part B: Polym. Phys.* 2011, **49**, 1051-1083.
- 21 W. M. Gramlich, M. L. Robertson and M. A. Hillmyer, *Macromolecules* 2010, **43**, 2313-2321.
- 22 W. J. Song, H. Z. Liu, F. Chen and J. W. Zhang, *Polymer* 2012, **53**, 2476-2484.
- 23 R. M. Michell, A. J. Müller, A. Boschetti-de-Fierro, D. Fierro, V. Lison, J.-M. Raquez and P. Dubois, *Polymer* 2012, **53**, 5657-5665.
- 24 H. T. Oyama, *Polymer* 2009, **50**, 747-751.
- 25 G.-C. Liu, Y.-S. He, J.-B. Zeng, Y. Xu and Y.-Z. Wang, *Polym. Chem.* 2014, **5**, 2530-2539.
- 26 Y. S. He, J. B. Zeng, G. C. Liu, Q. T. Li and Y. Z. Wang, *RSC Adv.* 2014, **4**, 12857-12866.
- 27 H. Fang, F. Jiang, Q. Wu, Y. Ding and Z. Wang, *ACS Appl. Mater. Inter* 2014, **6**, 13552-13563.
- 28 J. Park, S. Hwang, W. Yoon, E. Yoo and S. Im, *Macromol. Res.* 2012, **20**, 1300-1306.
- 29 A. Ranade, N. D'Souza, C. Thellen and J. A. Ratto, *Polym. Int.* 2005, **54**, 875-881.
- 30 W.-R. Jiang, R.-Y. Bao, W. Yang, Z.-Y. Liu, B.-H. Xie and M.-B. Yang, *Mater. Design* 2014, **59**, 524-531.
- 31 X. Wang, W. Liu, H. Zhou, B. Liu, H. Li, Z. Du and C. Zhang, *Polymer* 2013, **54**, 5839-5851.
- 32 S. F. Edwards, H. Takano and E. M. Terentjev, *J. Chem. Phys.* 2000, **113**, 5531-5538.
- 33 C. Liu, J. Wang and J. He, *Polymer* 2002, **43**, 3811-3818.

-
- 34 J. Honerkamp and J. Weese, *Rheol. Acta* 1993, **32**, 65-73.
- 35 S. T. Milner and T. C. B. McLeish, *Macromolecules* 1997, **30**, 2159-2166.
- 36 R. C. Ball and T. C. B. McLeish, *Macromolecules* 1989, **22**, 1911-1913.
- 37 D. Maier, A. Eckstein, C. Friedrich and J. Honerkamp, *J. Rheol.* 1998, **42**, 1153-1173.
- 38 S. I. Woo, B. O. Kim, H. S. Jun and H. N. Chang, *Polym. Bull.* 1995, **35**, 415-421.
- 39 W. Zhong, J. J. Ge, Z. Y. Gu, W. J. Li, X. Chen, Y. Zang and Y. L. Yang, *J. Appl. Polym. Sci.* 1999, **74**, 2546-2551.
- 40 Y. Di, S. Iannace, E. Di Maio and L. Nicolais, *Macromol. Mater. Eng.* 2005, **290**, 1083-1090.
- 41 R. Bhardwaj and A. K. Mohanty, *Biomacromolecules* 2007, **8**, 2476-2484.

Graphical Abstract

Balanced strength and ductility improvement of in situ crosslinked polylactide/poly(ethylene terephthalate glycol) blends*Rui-Ying Bao, Wen-rou Jiang, Zheng-Ying Liu, Wei Yang, Bang-Hu Xie, Ming-Bo Yang*